

Dynamics of DNA replication: an ultrastructural study

Anatoly A. Philimonenko^a, Dean A. Jackson^b, Zdeněk Hodný^a, Jirí Janáček^c,
Peter R. Cook^d, Pavel Hozák^{a,*}

^a Institute of Experimental Medicine, Academy of Sciences of the Czech Republic, Vídeňská 1083, 142 20 Prague 4 – Krč, Czech Republic

^b Department of Biomolecular Sciences, UMIST, P.O. Box 88, Manchester M60 1QD, UK

^c Department of Biomathematics, Institute of Physiology, Academy of Sciences of the Czech Republic, Prague, Czech Republic

^d Sir William Dunn School of Pathology, University of Oxford, South Parks Road, Oxford OX1 3RE, UK

Received 22 March 2004, and in revised form 23 July 2004

Available online 29 September 2004

Abstract

DNA replication in cells takes place in domains scattered throughout the nucleoplasm. We have characterized the dynamics of DNA synthesis in synchronized mid-S-phase HeLa cells. Saponin-permeabilized cells were allowed to elongate nascent DNA chains in presence of biotin-dUTP for 5, 15, and 30 min (a pulse experiment), or for 5 min followed by an incubation with unlabeled precursors for 10 or 25 min (a pulse-and-chase experiment). The replication foci were then identified in ultrathin sections using immunogold labeling of the incorporated biotin. Total number of particles per nucleus, total scanned area of the nucleus, size, shape, and gold particle number of each labeled cluster, and the density of clusters per nucleus were evaluated. We have demonstrated that as replication proceeds, the labeled sites increase in size up to 240 nm (30 min incorporation) while maintaining a broadly round shape. In pulse-and-chase experiments the labeled DNA was shown to spread to occupy DNA foci of ~400 nm in diameter. These results demonstrate that DNA replication is compartmentalized within cell nuclei at the level of DNA foci and support the view that the synthetic centers are spatially constrained while the chromatin loops are dynamic during DNA synthesis.

© 2004 Elsevier Inc. All rights reserved.

Keywords: DNA replication; Nucleoskeleton; Replication factories; Replication foci; Chromosome

1. Introduction

It is accepted that the mammalian nucleus, despite an absence of intranuclear membranes, is organized into functional domains or foci, where nuclear processes like DNA replication, transcription, RNA processing and ribosome biogenesis take place (Henzel et al., 2001; Jackson, 2003; Scheer and Weisenberger, 1994; Spector, 2001; Stein et al., 2003; van Driel and Fransz, 2004). For example, domains of active DNA synthesis that are scattered throughout the nucleoplasm during S-phase contain replication proteins such as DNA polymerases and proliferating cell nuclear antigen—PCNA (Hozák

et al., 1993; Sporbert et al., 2002) as well as proteins that regulate the cell cycle—such as cyclin A and cdk2 (Cardoso et al., 1993)—and chromatin structure—such as uracil-DNA glycosylase (Otterlei et al., 1999) and DNA methyltransferase (Leonhardt et al., 1992). The existence of localized replication domains appears to be a common architectural theme as these structures are found in species ranging from mammals (Hozák et al., 1993; Nakamura et al., 1986; Nakayasu and Berezney, 1989) to plants (Sparvoli et al., 1994). Perhaps surprisingly, the theme may even apply in prokaryotes, as the active *Bacillus subtilis* DNA polymerase complexes were found to be localized in fixed intracellular positions (Lemon and Grossman, 1998). Also, no fundamental differences were found in the spatio-temporal organization of replication patterns between primary, immortal or

* Corresponding author. Fax: +420 241 062 219.

E-mail address: hozak@biomed.cas.cz (P. Hozák).

transformed mammalian cells (Dimitrova and Berezney, 2002).

Replication domains in animal cells were first described in the pioneering experiments of Nakamura et al. (1986). In this study, rodent fibroblast were shown to have about 100 sites of active DNA synthesis, which grew in size for about an hour before new active sites were activated at adjacent nuclear positions. More recent reports have used improved imaging techniques to estimate that both mouse 3T3 cells (Ma et al., 1998) and HeLa cells (Jackson and Pombo, 1998) contain ~1000 replication sites in early S-phase. As estimated by light microscopy, typical DNA foci are ~500 nm in size (Ma et al., 1998) and contain about 1 Mb DNA. During the early stage of S-phase, average replicons are ~150 kb in size. This is consistent with the view that each replication site must contain 5–6 replicons in order to complete synthesis in the observed time frame of 45–60 min given that replication proceeds at a rate of about 1.5 kb/min (Jackson and Pombo, 1998; Ma et al., 1998). Importantly, these groups of replicons appear to remain stably associated within DNA foci over at least 10 cell generation (Jackson and Pombo, 1998; Ma et al., 1998; Zink et al., 1998) suggesting that they may be essential sub-units of chromosome structure. The kinetics of replication sites was also studied in cells of Hydra (Alexandrova et al., 2003). Following subsequent incorporations of IdU and CldU (chase 2 h), the resulting replication sites did not coincide; nevertheless, the replication pattern was similar.

This observation raises the possibility that DNA foci might be fundamental units of both chromosome structure and function. This notion is supported by the fact that distinct groups of DNA foci are replicated reliably at specific times of S-phase during subsequent cell cycles (Jackson and Pombo, 1998; Ma et al., 1998). Furthermore, the organization of DNA foci might also provide a mechanism that allows DNA synthesis to spread efficiently throughout the genome by virtue of a ‘domino’ effect whereby the completion of replication at a particular site will activate replication at spatially adjacent sites (Ma et al., 1998; Manders et al., 1996; Sporbert et al., 2002). In this way, the organization of DNA foci will define the replication program. In addition, many lines of evidence suggest that the active replication complexes of mammalian cells are tethered to an underlying framework called the nuclear matrix or nucleoskeleton (Hozák et al., 1993; Tubo and Berezney, 1987). If this is true, during DNA synthesis the DNA polymerase complexes must remain fixed and chromatin must move so that DNA is reeled through the active synthetic centers (Hozák and Cook, 1994; Jackson, 1990).

In fact, surprisingly little is known about the dynamic properties of chromatin during DNA synthesis even though this must be an essential feature of the replication process. Specialized approaches that allow large

chromosomal domains to be tagged and visualized in living cells suggest that large-scale chromatin movements might occur during S-phase (Li et al., 1998). However, within natural chromatin domains, chromatin dynamics appear to be locally constrained (Chubb et al., 2002); though this analysis does not rule out the possibility that chromatin might be highly dynamic at the level of DNA foci. In principle, it should be possible to establish the extent of chromatin movement in response to DNA synthesis from the distribution of nascent DNA with replication foci. Ma et al. (1998) used a spot-based segmentation analysis to investigate the architecture of replication foci using confocal microscopy. They demonstrated that the dimensions of individual replication sites changed little over labeling periods of 2–30 min, suggesting that the replication sites correspond to discrete domains of DNA whose replication occurs uniformly over the individual replication site.

In a recent study (Jaunin et al., 2000), classical immunoelectron microscopy techniques were used to show that nascent sites—detected using a 2 min pulse-label with BrdU—were localized to the diffuse chromatin of the perichromatin regions, often in the vicinity of perichromatin fibrils. During prolonged pulses and pulse-chase experiments the regions of dense chromatin adjacent to these perichromatin regions became labeled. When a pulse-chase-pulse approach was used to label the DNA with IdU and then CldU, the nascent label was found in the perichromatin zone, supporting the view that replication occurred within a defined nuclear zone and that the replicated DNA then moved into the adjacent chromatin-rich area. Earlier studies using a specialized technique that allowed cell structure to be preserved while removing almost all chromatin showed that early S-phase replication occurs within discrete replication ‘factories’ of 50–100 nm, and in larger ‘factories’ in mid- and late-S-phase (Hozák et al., 1993, 1994). Although these reports cannot be directly compared as they use so different techniques, they both support the hypothesis that replication occurs within a defined inter-chromatin compartment so that during replication DNA from the adjacent chromatin-rich compartment must be translocated to the active site at the border of the chromatin domain.

In the current report, we develop the argument that DNA movement during replication must be an essential part of the replication process. To explore this issue, we have undertaken a detailed analysis of the spread of DNA from the nascent replication sites. Nascent DNA was labeled with biotin-dUTP in permeabilized cells using pulse and pulse-chase strategies. This approach was taken for two specific reasons. First, when biotin-dUTP is used as the replication precursor the incorporated biotin can be detected in fixed cells using antibodies or streptavidin. BrdU, in contrast, can only be detected when the DNA is denatured, compromising both morphology and labeling efficiency. Second, in permeabilized

cells the concentrations of the precursor pools can be regulated so that the levels of modified precursor incorporated and overall elongation rates can be manipulated at will. Using immunogold procedure on ultrathin sections we show that the clusters of labeled nascent DNA grow gradually during replication while their shape remains essentially circular in cross-section. Our data support the view that replication occurs within discrete active sites and is not in agreement with the view that active replication complexes scan along the DNA during synthesis. Instead, replication seems to involve a cycle of DNA movement, where chromatin first moves from the chromatin-rich regions into the active site where replication occurs. Following synthesis and chromatin maturation, it is necessary that the daughter DNA molecules re-fold and move out of the active site to regenerate the chromatin-rich nuclear compartment.

2. Materials and methods

2.1. Cell culture and cell synchronization

Suspension cultures of human cervical carcinoma (HeLa) cells were grown in Eagle medium (S-MEM, Sigma, St. Louis, MO, USA) supplemented with 5% fetal calf serum (Sigma, St. Louis, MO, USA) at 37 °C. Cells were synchronized in S-phase using a thymidine block (Jackson and Cook, 1986), and then in mitosis by a nocodazole block (20 ng/ml nocodazole, Sigma, St. Louis, MO, USA) for 8 h. The inhibitors were removed by careful washing and the cells were re-grown. Cell samples were taken (about 5×10^6 cells per sample) 14 h after the release from mitosis, which corresponds to mid-S-phase, as shown previously (Hozák et al., 1994).

2.2. Cell permeabilization

Synchronized cells were collected, washed twice in phosphate-buffered saline (PBS), and permeabilized by 0.1 mg/ml saponin (Sigma, St. Louis, MO, USA) in “physiological” buffer (PB; 22 mM Na⁺, 130 mM K⁺, 1 mM Mg²⁺, <0.3 μM free Ca²⁺, 67 mM Cl⁻, 65 mM CH₃COO⁻, 11 mM phosphate, 1 mM ATP, 1 mM dithiothreitol, and 0.1 mM phenylmethylsulphonyl fluoride, pH 7.4) for 3 min at 0 °C. Cell membrane integrity was monitored using trypan blue (Merck). More than 90% of HeLa cells remained permeabilized for at least 1 h, so that under the experimental conditions used, the labeled precursors had intracellular access during the whole time of nucleotide incorporation (5–30 min).

2.3. Replication *in vitro*

After saponin permeabilization, cells were rinsed with two changes of ice-cold PB. A prewarmed 10× concen-

trated replication mix was added to permeabilized cells to give final concentrations of 100 μM CTP, UTP, and GTP, 250 μM dCTP, dATP, and dGTP, plus 100 μM biotin-16-dUTP (biotin-dUTP) and 2.15 mM MgCl₂ in PB. For pulse experiments, the nucleotide incorporation reaction was stopped with 10 volumes of ice-cold PB after 5, 15, and 30 min of incubation at 33 °C (experimental groups 1, 2, and 3, respectively). In pulse and chase experiments, cells were incubated in replication solution in the presence of biotin-dUTP for 5 min, washed in PB, and then allowed to replicate in the presence of unlabeled precursors for 10 and 25 min (experimental groups 4 and 5). The reaction was stopped with 10 volumes of ice-cold PB.

2.4. Dynamics of dNTP incorporation

The dynamics of dTTP incorporation in the presence and in the absence of biotin-labeled precursors was studied quantitatively using the incorporation of [³²P]dTTP. Cells were permeabilized with saponin and then rinsed twice with ice-cold PB. A prewarmed 10× concentrated replication mix was then added to permeabilized cells to give final concentrations of 100 μM CTP, UTP, and GTP, 250 μM dCTP, dATP, and dGTP, 2.15 mM MgCl₂, 100 μM biotin-16-dUTP, and [³²P]dTTP (~3000 Ci/mmol, 10–20 μCi/ml, Amersham). In pulse experiments the reaction was stopped after 5, 15, and 30 min of incubation at 33 °C by addition of an equal volume of 2% SDS. Samples were then incubated for 2 h at 37 °C. ³²P incorporation into the acid-insoluble fraction of cell lysate was measured by scintillation counting (Packard 300 CD) (Jackson and Cook, 1986). In pulse-and-chase experiments, cells were washed after 5 min of replication in the presence of biotin-dUTP and then allowed to replicate in the presence of unlabeled precursors and [³²P]dTTP for 10 and 25 min. The following procedure was the same as in pulse experiment. The results of measurements are expressed as pmol of incorporated TMP per 10⁶ cells and as thousands of incorporated dNMP per replication fork.

2.5. Electron microscopy and image capture

Following DNA replication in permeabilized HeLa cells, the cells were fixed at 0 °C in 3% paraformaldehyde and 0.1% glutaraldehyde in Sørensen buffer (SB; 0.1 M sodium/potassium phosphate buffer, pH 7.3) for 30 min, washed twice in SB (10 min each), and then resuspended in 1% low-melting point agarose (Sigma, St. Louis, MO, USA) in SB at 37 °C. Cells were then pelleted and the solidified pellet cut into small pieces. The pieces were dehydrated in series of ethanol solutions with increasing concentration of ethanol. The ethanol was then replaced in two steps by LR White resin (Polysciences, Warrington, USA) and the resin was

polymerized for five days at -20°C under UV light. After cutting 80 nm sections, non-specific labeling was blocked by preincubation with 10% normal goat serum, 1% BSA, and 0.1% Tween 20 in PBS for 30 min at room temperature. For the detection of nascent DNA, the sections were incubated with 10 nm gold-conjugated goat antibodies to biotin (British BioCell International, Cardiff, UK), washed twice in PBT (0.005% Tween 20 in PBS), twice in water and air-dried. Finally, sections were contrasted with a saturated solution of uranyl acetate in water for 4 min and observed in a Philips CM100 electron microscope (Philips, Eindhoven, The Netherlands) equipped with a CCD camera (Model 673, GATAN, USA). For statistical analysis of clustering patterns of the gold particles, series of digital electron microscope images of nuclear sections were taken from about 20 cells per experimental group. In order to take into account only mid-S-phase cells, we chose only cells in which the nucleoplasm contained clusters of gold particles spread throughout the whole extranucleolar region (as immunofluorescence had previously shown that replication sites in mid-S-phase, are homogeneously distributed throughout nucleoplasm; Hozák et al., 1994).

2.6. Image analysis and statistical evaluation

The clustering of gold particles was estimated using a macro developed for LUCIA image-processing software (Laboratory Imaging, Prague, Czech Republic). Each particle was identified, and the clusters of particles were defined. Two particles were regarded as forming a cluster if the distance between them was less than 80 nm. The area of a cluster, number of particles inside it and its circularity and elongation factors were calculated. The circularity factor (CF) is

$$\text{CF} = \frac{4\pi \times \text{area}}{\text{Perimeter} \times \text{perimeter}}$$

It equals 1 for circles; all other shapes have a value lower than 1. The elongation factor (EF) is

$$\text{EF} = \frac{\text{Max_projected diameter}}{\text{Min_projected diameter}}$$

It equals 1 for circles, and all other shapes have a value higher than 1. The statistical significance of experimental values was tested using the non-parametric Kolmogorov–Smirnov two-sample test.

Theoretically, one might expect that the CF and EF values could be biased in the case when only a few gold particles decorate one replication focus. We compared therefore the experimental values of CF and EF with those of randomly generated clusters of gold particles. For random generation, convex hulls of n (pseudo)random points were used (10^6 repetitions, random generator after L'Ecuyer with Bays-Durham shuffle; Press et al., 1999). Two possibilities were examined: clusters

were generated either within a circle, or within an ellipse (ratio of semiaxes = 2).

The numbers of clusters per μm^2 of the nucleoplasm (cluster densities) in each experimental group were also calculated, and used to estimate the total number of clusters per nucleus according to Weibel (1979)

$$N_V = \frac{N_A}{D + t},$$

where N_V is number of structures per investigated volume, N_A is the cluster density, D is the diameter of structures, and t is the section thickness, i.e., 80 nm. The total number of replication clusters per nucleus N is then calculated using the total nuclear volume V

$$N = N_A \times V.$$

3. Results

3.1. An effect of biotin-dUTP on replication rate

We first characterized how the presence of biotin-dUTP influences the incorporation dynamics of dNTPs into DNA in permeabilized HeLa cells. The curve with triangles in Fig. 1 demonstrates that the presence of biotin-dUTP reduces the rate of incorporation of radioactively labeled dNTPs by about 50% during the first 5 min. However, the character of the curve for dNTPs incorporation is similar in the absence or in the presence of labeled precursors. In pulse-chase experiments (i.e., when biotin-dUTP was removed after 5 min and then cells allowed to replicate in the presence of only natural precursors), the rate fully recovered and reached the control level in less than 10 min (Fig. 1).

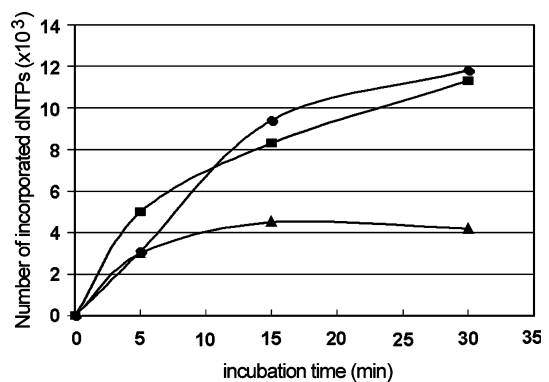


Fig. 1. The dynamics of biotin-dUTP incorporation. Permeabilized HeLa cells were allowed to replicate in the presence of $[^{32}\text{P}]\text{dTTP}$ for different times. Triangles, dNTP incorporation in the presence of biotin-dUTP. Squares, dNTP incorporation in absence of biotin-dUTP. Ellipses, after 5 min replication in biotin-dUTP, cells were washed and allowed to replicate with untagged precursors. All three curves have similar shapes.

3.2. Distribution of nascent DNA

The distribution of incorporated biotin-dUTP was analyzed in detail using electron microscopy of immunogold-labeled ultrathin sections. Biotin-dUTP was labeled with goat anti-biotin antibodies conjugated to 10 nm gold particles. The majority of label is clearly incorporated as clusters of gold particles in the nucleoplasm (Fig. 2). These clusters were of different sizes and contained different number of gold particles (Figs. 2A–D, arrows; Figs. 3A and B, curves with squares). After replication for 5 min, only small clusters can be found (Fig. 2A). However, after 15 and 30 min the clusters become significantly larger (Figs. 2B and C). In pulse-chase experiments, the clusters are similar after a 5 min pulse and 25 min chase to those labeled during a 30 min pulse (Fig. 2D). However, the clusters after 25 min chase are more dispersed (1043.8 ± 579.4 particles/ μm^2) than after 30 min pulse (1234.5 ± 650.5 particles/ μm^2 ; compare also Figs. 2C and D). The dynamics of gold particles incorporation into clusters is similar to the incorporation of radioactively labeled precursors into permeabilized cells (compare Fig. 3A, the curve with squares and Fig. 1).

Single gold particles were also found in all experimental groups (Figs. 2A–D). However, the total number of single particles did not significantly change during biotin-dUTP pulse incorporation and was comparable in all experimental groups (Figs. 3A and B, curves with triangles). These experimental data support previous observations using bromodeoxyuridine that replication takes place in clusters/foci (Nakamura et al., 1986; Nakayasu and Berezney, 1989).

Evaluation of cluster area and of the number of particles in each particular cluster demonstrated that the amount of clusters with large numbers of gold particles (more than 7) increases along the pulse length. A decrease in the number of large clusters was seen if the pulse was followed by a chase (compare plots B and D in Fig. 4). Presumably, some incorporated label spreads out beyond the original cluster. The label would then yield either single particles or particles belonging to a different cluster. Similarly, the proportion of clusters, which occupy areas larger than $0.015 \mu\text{m}^2$ slightly increases with the length of pulse from 5 to 30 min (Figs. 5A and B). In contrast, in pulse-chase experiments the proportion of larger clusters remained similar while increasing the length of the chase from 10 to 25 min (Figs. 5C and D).

The direct correlation between the area occupied by a cluster and the number of particles inside this cluster shows that both parameters change simultaneously with the extent of replication (Fig. 6). In pulse experiments, the number of large clusters of more than $0.015 \mu\text{m}^2$ with seven and more gold particles increased with the length of the pulse (see Figs. 6A–C). However,

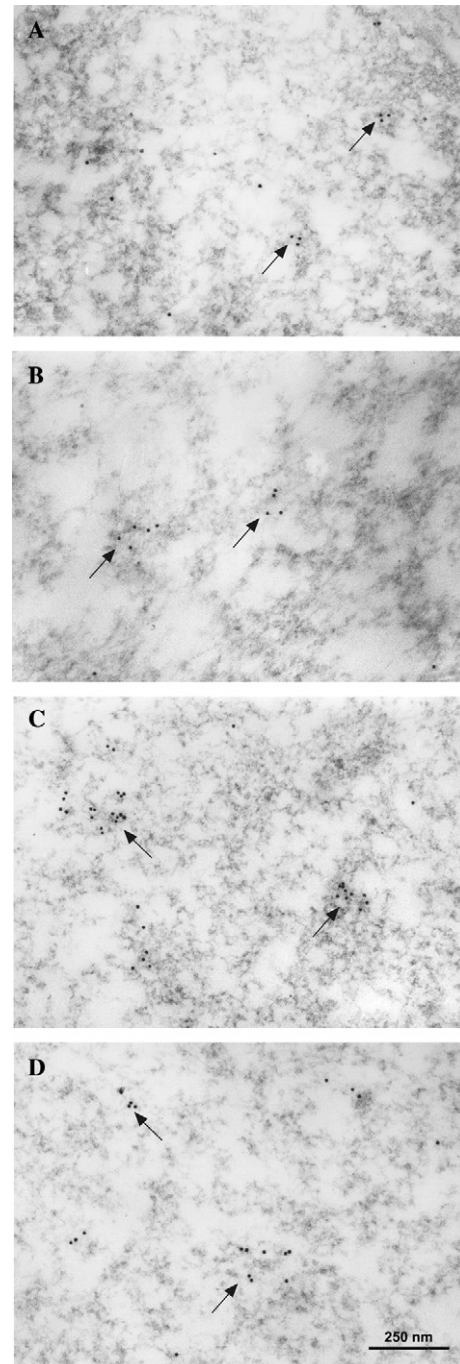


Fig. 2. DNA replication takes place focally. Nascent DNA in sections of HeLa cell nuclei was labeled with 10 nm gold particles. The label is found as single particles and as clusters of gold particles (arrows). (A) 5 min; (B) 15 min; (C) 30 min pulse; and (D) 5 min pulse and 25 min chase. Bar, 250 nm.

in pulse-chase experiments, the pattern did not change significantly with the length of the chase (Figs. 6D and E).

The clusters which occupy an area larger than $0.02 \mu\text{m}^2$ and which consist of more than 12 gold particles appear only after 30 min (Fig. 6C). However, such clusters are already present after a 5 min pulse and

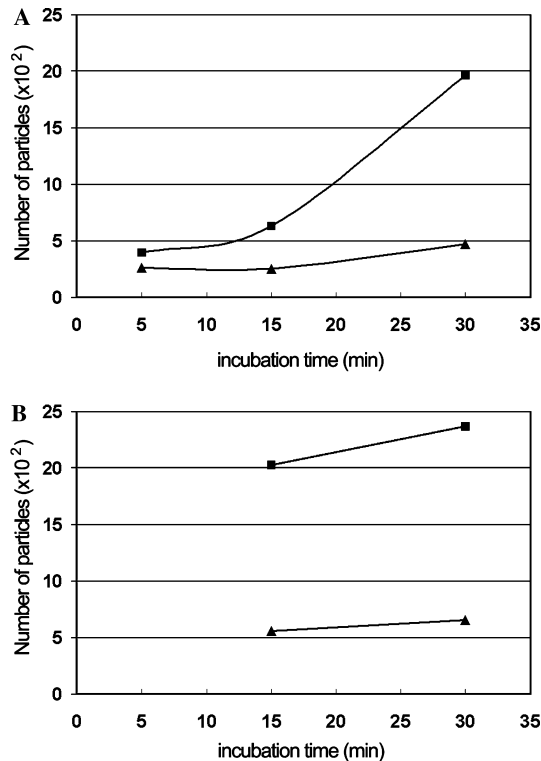


Fig. 3. Most label of nascent DNA localizes to immunogold clusters. Total number of gold particles per entire evaluated area was estimated in experiments like shown in Fig. 2. The particles belong to two classes: single particles, and particles that create clusters. (A) Pulse of 5, 15, or 30 min and (B) pulse-chase (5 min pulse plus 10 or 25 min chase). Squares, gold particles in clusters. Triangles, single gold particles. The number of single particles does not change with incubation time (so they represent background labeling), while the number of particles in clusters increases (so they reflect DNA synthesis).

10 min chase (compare plots C and D in Fig. 6). This is in agreement with the radiolabeling experiment, which demonstrated an inhibition by biotin-dUTP during the pulse followed by a full recovery in 10 min after removing the labeled precursor (Fig. 1).

The density of clusters with five or more gold particles in the nucleoplasm increased gradually between 5 and 30 min to 0.25 clusters/ μm^2 . Using the known nuclear volume and standard stereological procedures, we then calculate that there are ~ 800 clusters per nucleus. In pulse-chase experiments, the density of clusters with five or more gold particles was 0.4 clusters/ μm^2 after 5 min of pulse and 10 min of chase, and 0.3 after 5 min of pulse, and 25 min of chase.

The circularity and elongation factors can be used to provide an estimate of the general shape of a cluster, and how it might change during a pulse-chase (see Section 2 for details). During both pulse and pulse-chase labelings, the clusters had circularity factors of about 0.75 and elongation factors of about 2 (Table 1). This is consistent with a generally round/ellipsoid shape that remained so as the clusters grew in size.

3.3. Stereological considerations

It follows from the classical solution of the Sylvester problem that in the case of low gold labeling density, the shape and size of the clusters could be biased (Kendall and Moran, 1963). Indeed, the mean area of a triangle created with three randomly placed points inside a circle covers only about 7% of the circle area. In order to assess this possible bias, we calculated the elongation and circularity factors of the artificially created clusters using Monte-Carlo simulations of gold particles randomly generated inside the expected round/ellipsoid structures (replication foci). The results given in Table 1 clearly show that the theoretical clusters (mostly those with a small number of gold particles) are much more elongated than in our experiments. For example, clusters containing three gold particles had CF of ~ 0.7 and EF of ~ 2 , while the calculated parameters were ~ 0.34 and ~ 3.3 , respectively. In other words, the replication foci probably are in reality even more circular than if we rely on the detected shape of immunogold clusters. One possible explanation is a repulsion of gold particles at very short distances (Humbel and Biegelmann, 1992) that neutralizes the above-described bias.

4. Discussion

In proliferating cells, DNA synthesis must be controlled with absolute precision so that each base pair of DNA is replicated once but only once in every cell cycle. In mammals, while some critical regulatory features have been described, other aspects of the process that ensure regulated synthesis remain unknown (Berezney et al., 2000; Gilbert, 2002). In particular, very little is known about the molecular mechanisms that regulate the activation of replication from defined regions of the genome throughout S-phase. The best models that have been developed to address this issue involve groups of replicons within DNA foci that behave as structurally stable replicating units (Cremer and Cremer, 2001). S-phase progression would then occur by virtue of a domino-like effect wherein events that occur during the replication of one structural unit lead to changes in an adjacent unit which will allow synthesis to proceed. In this model, spatial parameters of chromosome architecture define the S-phase program.

The basic features required by this model have been characterized in detail. Numerous studies have demonstrated that DNA replication takes place in replication domains or foci and that defined groups of foci are replicated at specific times of S-phase so that characteristic patterns of synthesis define S-phase stage (Humbert and Usson, 1992; Nakamura et al., 1986; Nakayasu and Berezney, 1989; O'Keefe et al., 1992). DNA foci are also known to contain groups of replicons that are replicated

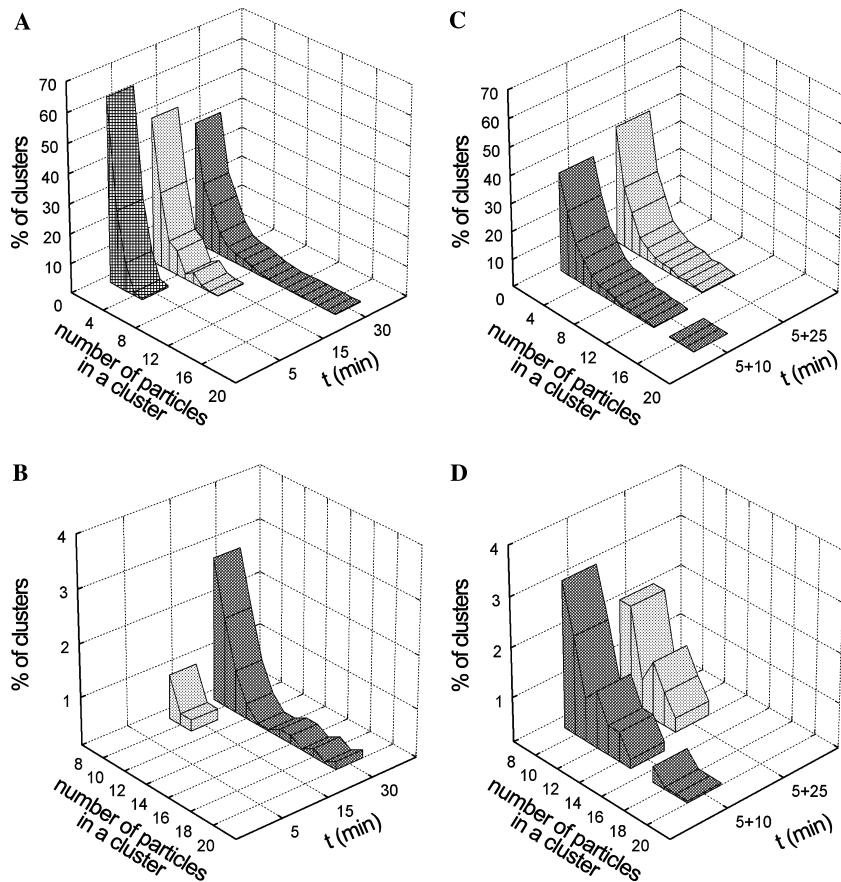


Fig. 4. Distribution of clusters according to the number of gold particles in experiments like shown in Fig. 2. The number of particles in each particular cluster was counted, and the percentages of clusters containing different numbers of gold particles were calculated. (A) Pulse of 5, 15, or 30 min; (B) detail of (A) (note that here we start with clusters containing eight particles); (C) 5 min pulse followed by 10 or 25 min chase; and (D) detail of (C).

together and form stable structural cohorts over many cell division cycles (Jackson and Pombo, 1998; Ma et al., 1998; Zink et al., 1998). Foci that are replicated later within S-phase appear to arise at sites adjacent to foci that have recently completed synthesis (Manders et al., 1996; Sporbert et al., 2002). Two critical issues remain unresolved. First, the micro-architecture of DNA foci has not been studied in detail, and reports on the distribution of synthetic sites within the foci are conflicting (see Section 1). Second, little is known about the movement and distribution of nascent DNA within foci during DNA synthesis.

Most studies that have been designed to analyze DNA foci have used light microscopy and so suffer from limitations of resolution. At the ultrastructural level, two types of synthetic sites can be distinguished: the electron-dense structures (or replication bodies), and others that lack a distinct ultrastructure and which can be visualized only by immunodetection of incorporated precursors (Hozák et al., 1993, 1994). In this study, we describe the dynamics of replication during mid-S-phase of the cell cycle that takes place inside replication domains, which have no distinct underlying (dense) structure.

In permeabilized cells, replication in the presence of biotin-dUTP is known to be less efficient than in the presence of an equivalent concentration of dTTP (Hozák et al., 1993, 1994). Nevertheless, biotin-dUTP supports elongation with kinetics that reflects those obtained using only the natural precursor (see the shapes of the curves in Fig. 1). Immunogold labeling demonstrates highly similar kinetics (compare Fig. 3A, curve with squares and Fig. 1) suggesting it provides a suitable method of monitoring DNA synthesis whilst allowing high spatial resolution.

We have demonstrated using both pulse or pulse-chase strategies that most (i.e., >90%) nascent DNA (see e.g., Fig. 2C) is synthesized in discrete foci marked by clusters of gold particles against a background of single particles. The total number of single particles was the same in all experimental groups and clearly presents background labeling. In contrast, the number of particles in clusters increased in proportion to the amount of biotin incorporated. This confirms results obtained using light microscopy (Jackson and Pombo, 1998; Ma et al., 1998; Nakamura et al., 1986; Zink et al., 1998). About 800 replication sites per nucleus are seen after a

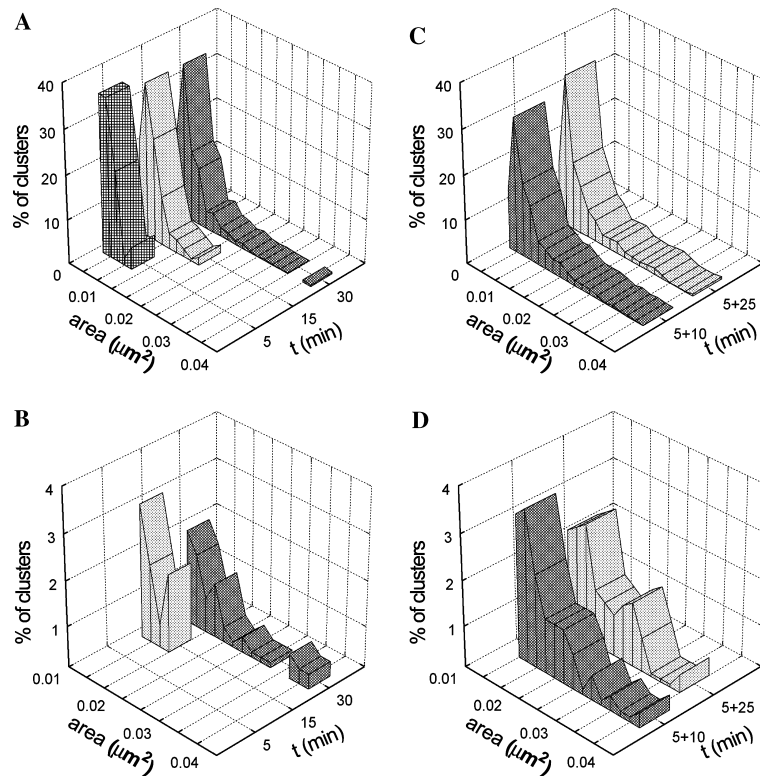


Fig. 5. Distribution of clusters according to their area in experiments like shown in Fig. 2. The area of each particular cluster was measured and the percentages of clusters with different areas calculated. (A) Pulse of 5, 15, or 30 min; (B) detail of (A) (note that here we start with cluster areas of $0.01 \mu\text{m}^2$); (C) 5 min pulse followed by 10 or 25 min chase; and (D) detail of (C).

30 min pulse. This confirms recent estimates that both mouse 3T3 (Ma et al., 1998) and HeLa cells (Jackson and Pombo, 1998) contain ~ 1000 sites in early S-phase.

As the length of a pulse increases (or when a pulse is followed by a chase) the clusters enlarge but remain roughly circular in shape (Figs. 2C and D). This is consistent with replication taking place in a limited region (focus) and with newly replicated DNA moving away from the synthetic site. On the other side, these data are inconsistent with the view that replication foci operate as replication centers that perform DNA synthesis on stretched chromatin fibers.

Sectioning of elongated object, e.g., prolate spheroid yields sections of various shapes, from circular to those elongated as the original object. In less elongated objects (e.g., 2:1), the frequencies of all shapes are similar, while sectioning strongly elongated object (e.g., 5:1) yields a large proportion of circular sections and smaller number of largely elongated sections (Cruz-Orive, 1978; Ohser and Muecklich, 2000). In both cases, the elongated sections are remarkable. However, in our experiments we detected only clusters with the maximal EF of ~ 3.5 and minimal CF of ~ 0.5 for clusters with more than five gold particles. This means that we never observed stretched fibers of nascent DNA/chromatin.

The size of clusters obtained in our experiments is also of interest. The length of the DNA in a chromatin loop in

a HeLa cell is about 8.6×10^4 bp (Jackson et al., 1990); if packed as a 30 nm chromatin fiber this would correspond to a physical length of ~ 480 nm. During the maximal time of replication in our experiments about 1.2×10^4 bp was replicated (see Fig. 1), equivalent to ~ 140 nm packed into a 30 nm fiber. This compares with a mean radius of 180 nm of the largest clusters seen after 30 min. Therefore nascent DNA remains close to the synthetic site where, under these conditions, it is confined with DNA foci of up to 400 nm in diameter. The focal structure is preserved during the course of the experiment and no local restructuring of the foci is seen even though some sites will terminate replicating during the course of labeling in these cell populations. These results are consistent with the view that replication takes place in distinct factories (Hozák et al., 1993) but also supports similar observation using electron microscopy that has shown DNA replication to occur at the surface of dense chromatin regions within the perichromatin compartment (Jaunin et al., 2000). From this report, it is clear that within DNA compartments (of the size of DNA foci) replication occurs within a peripheral zone and does not at any time spread into the DNA-rich compartment itself. This is consistent with the view that a synthetic compartment is assembled within the inter-chromatin region, where it could be associated with the nucleoskeleton, and that the chromatin must translocate into the active site and the replicated daughter

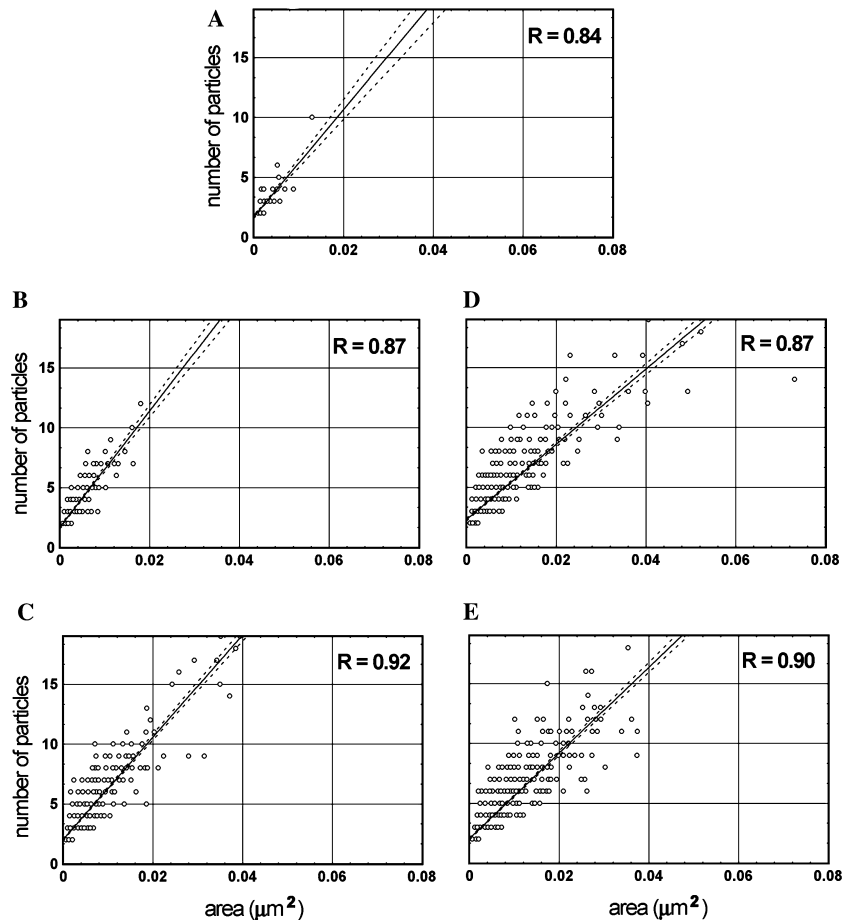


Fig. 6. The cluster area and number of particles in them correlate. Each plot represents one experimental group. A, B, and C correspond to 5, 15, and 30 min pulses, respectively. D and E correspond to 5 min pulse and 10 and 25 min chases, respectively. The absence of clusters with small area but large numbers of particles demonstrates the direct correlation between the area occupied by a cluster and its number of gold particles. R, correlation coefficient.

Table 1

Comparison of circularity (CF) and elongation (EF) factors of experimental (CF_{EXP} and EF_{EXP}) and randomly generated (CF_{T} and EF_{T}) clusters of gold particles

Experiment	N_{C}	N_{gp}	CF			EF		
			$CF_{\text{EXP}} \pm \text{SD}$	CF_{T}		$EF_{\text{EXP}} \pm \text{SD}$	EF_{T}	
				Generated for circle	Generated for ellipse		Generated for circle	Generated for ellipse
5 min pulse	59	3.5	0.69 ± 0.127	0.34	0.31	2.31 ± 0.932	3.33	3.85
15 min pulse	165	4.2	0.69 ± 0.123	0.50	0.44	2.32 ± 0.880	2.38	2.94
30 min pulse	468	4.9	0.70 ± 0.121	0.59	0.51	2.23 ± 0.822	2.04	2.56
5 min pulse + 10 min chase	464	5.1	0.69 ± 0.125	0.59	0.51	2.30 ± 0.992	2.04	2.56
5 min pulse + 25 min chase	600	5.0	0.68 ± 0.116	0.59	0.51	2.30 ± 0.812	2.04	2.56

Note. The CF of ~ 0.7 and EF of ~ 2.3 indicate that the clusters containing nascent DNA are always round/ellipsoid. As the CF and EF values could be biased when only low number of gold particles defines a cluster, a comparison of experimental and theoretical values is also given. Note that both CF and EF are very stable during dNTP incorporation in all experimental groups. They represent more circular shape of the experimental gold particle clusters than randomly generated (see Section 2). N_{C} , the total number of evaluated clusters; N_{gp} , the mean number of gold particles per cluster.

strands move back into the chromatin compartment as replication proceeds.

Models of this type are supported by the analysis of living cells expressing replication proteins tagged with

green fluorescent protein (GFP; Leonhardt et al., 2000; Sporbert et al., 2002). GFP-PCNA (proliferating cell nuclear antigen) provides an outstanding example. In non-S-phase cells GFP-PCNA is spread diffusely throughout

the nucleus but during S-phase a proportion of the previously soluble protein is assembled into the active replication centers which have a sufficiently high local density of GFP-PCNA molecules for them to be seen against the diffuse pools. This study supports the earlier observation that consecutive phases of DNA synthesis during S-phase are seen to take place within spatially adjacent or overlapping DNA foci (Manders et al., 1992, 1996). In this case, nascent DNA moves *in vivo* relative to the domains where replication takes place with a rate that is on the order of 0.5 $\mu\text{m}/\text{h}$; similar rates were seen during early and late S-phase (Manders et al., 1996).

In conclusion, we present a high-resolution study of the distribution of nascent DNA that demonstrates that DNA synthesis is restricted to a limited region of DNA foci rather than being dispersed throughout the actively replicating structures. This is consistent with the view that DNA synthesis occurs within defined nuclear compartments that represent the active replication centers (Hozák et al., 1993; Sporbert et al., 2002). It requires that chromatin must move from DNA-rich areas to engage the active site prior to synthesis. This is consistent with the observation that replication occurs at the peri-chromatin region at the periphery of dense chromatin (Jaunin et al., 2000).

Acknowledgments

We thank The Wellcome Trust (UK) and the Grant Agency of the Academy of Sciences of the Czech Republic (Grant Reg. No. IAA5039202) for support. This work was also supported by the institutional Grant No. AV0Z5039906 (P.H.) and BBSRC (UK). We are grateful to Dr. Lucie Kubínová for invaluable help with stereological evaluations.

References

- Alexandrova, O., Solovei, I., Cremer, T., David, C.N., 2003. Replication labeling patterns and chromosome territories typical of mammalian nuclei are conserved in the early metazoan Hydra. *Chromosoma* 112, 190–200.
- Berezney, R., Dubey, D.D., Huberman, J.A., 2000. Heterogeneity of eukaryotic replicons, replicon clusters, and replication foci. *Chromosoma* 108, 471–484.
- Cardoso, M.C., Leonhardt, H., Nadal-Ginard, B., 1993. Reversal of terminal differentiation and control of DNA replication: cyclin A and Cdk2 specifically localize at subnuclear sites of DNA replication. *Cell* 74, 979–992.
- Chubb, J.R., Boyle, S., Perry, P., Bickmore, W.A., 2002. Chromatin motion is constrained by association with nuclear compartments in human cells. *Curr. Biol.* 12, 439–445.
- Cremer, T., Cremer, C., 2001. Chromosome territories, nuclear architecture and gene regulation in mammalian cells. *Nat. Rev. Genet.* 2, 292–301.
- Cruz-Orive, L.-M., 1978. Particle size-shape distributions: the general spheroid problem. II. Stochastic model and practical guide. *J. Microsc.* 112, 153–167.
- Dimitrova, D.S., Berezney, R., 2002. The spatio-temporal organization of DNA replication sites is identical in primary, immortalized and transformed mammalian cells. *J. Cell Sci.* 115, 4037–4051.
- Gilbert, D.M., 2002. Replication timing and transcriptional control: beyond cause and effect. *Curr. Opin. Cell. Biol.* 14, 377–383.
- Henzel, M.J., Kruhlak, M.J., MacLean, N.A., Boisvert, F., Lever, M.A., Bazett-Jones, D.P., 2001. Compartmentalization of regulatory proteins in the cell nucleus. *J. Steroid Biochem. Mol. Biol.* 76, 9–21.
- Hozák, P., Cook, P.R., 1994. Replication factories. *Trends Cell Biol.* 4, 48–52.
- Hozák, P., Jackson, D.A., Cook, P.R., 1994. Replication factories and nuclear bodies: the ultrastructural characterization of replication sites during the cell cycle. *J. Cell Sci.* 107, 2191–2202.
- Hozák, P., Hassan, A.B., Jackson, D.A., Cook, P.R., 1993. Visualization of replication factories attached to nucleoskeleton. *Cell* 73, 361–373.
- Humbel, B.M., Biegelmann, E., 1992. A preparation protocol for postembedding immunoelectron microscopy of *Dictyostelium discoideum* cells with monoclonal antibodies. *Scanning Microsc.* 6, 817–825.
- Humbert, C., Usson, Y., 1992. Eukaryotic DNA replication is a topographically ordered process. *Cytometry* 13, 603–614.
- Jackson, D.A., 1990. The organization of replication centers in higher eukaryotes. *Bioessays* 12, 87–89.
- Jackson, D.A., 2003. The principles of nuclear structure. *Chromosome Res.* 11, 387–401.
- Jackson, D.A., Cook, P.R., 1986. A cell-cycle-dependent DNA polymerase activity that replicates intact DNA in chromatin. *J. Mol. Biol.* 192, 65–76.
- Jackson, D.A., Pombo, A., 1998. Replicon clusters are stable units of chromosome structure: evidence that nuclear organization contributes to the efficient activation and propagation of S phase in human cells. *J. Cell Biol.* 140, 1285–1295.
- Jackson, D.A., Dickinson, P., Cook, P.R., 1990. The size of chromatin loops in HeLa cells. *EMBO J.* 9, 567–571.
- Jaunin, F., Visser, A.E., Cmarko, D., Aten, J.A., Fakan, S., 2000. Fine structural *in situ* analysis of nascent DNA movement following DNA replication. *Exp. Cell Res.* 260, 313–323.
- Kendall, M.G., Moran, P.A.P., 1963. *Geometrical Probability*. Charles Griffin, London.
- Lemon, K.P., Grossman, A.D., 1998. Localization of bacterial DNA polymerase: evidence for a factory model of replication. *Science* 282, 1516–1519.
- Leonhardt, H., Page, A.W., Weier, H.U., Bestor, T.H., 1992. A targeting sequence directs DNA methyltransferase to sites of DNA replication in mammalian nuclei. *Cell* 71, 865–873.
- Leonhardt, H., Rahn, H.P., Weinzierl, P., Sporbert, A., Cremer, T., Zink, D., Cardoso, M.C., 2000. Dynamics of DNA replication factories in living cells. *J. Cell Biol.* 149, 271–280.
- Li, G., Sudlow, G., Belmont, A.S., 1998. Interphase cell cycle dynamics of a late-replicating, heterochromatic homogeneously staining region: precise choreography of condensation/decondensation and nuclear positioning. *J. Cell Biol.* 140, 975–989.
- Ma, H., Samarabandu, J., Devdhar, R.S., Acharya, R., Cheng, P.C., Meng, C., Berezney, R., 1998. Spatial and temporal dynamics of DNA replication sites in mammalian cells. *J. Cell Biol.* 143, 1415–1425.
- Manders, E.M., Stap, J., Brakenhoff, G.J., van Driel, R., Aten, J.A., 1992. Dynamics of three-dimensional replication patterns during the S-phase, analysed by double labelling of DNA and confocal microscopy. *J. Cell Sci.* 103, 857–862.
- Manders, E.M., Stap, J., Strackee, J., van Driel, R., Aten, J.A., 1996. Dynamic behavior of DNA replication domains. *Exp. Cell Res.* 226, 328–335.

- Nakamura, H., Morita, T., Sato, C., 1986. Structural organizations of replicon domains during DNA synthetic phase in the mammalian nucleus. *Exp. Cell Res.* 165, 291–297.
- Nakayasu, H., Berezney, R., 1989. Mapping replicational sites in the eucaryotic cell nucleus. *J. Cell Biol.* 108, 1–11.
- O’Keefe, R.T., Henderson, S.C., Spector, D.L., 1992. Dynamic organization of DNA replication in mammalian cell nuclei: spatially and temporally defined replication of chromosome-specific alpha-satellite DNA sequences. *J. Cell Biol.* 116, 1095–1110.
- Ohser, J., Muecklich, F., 2000. *Statistical Analysis of Microstructures in Material Science*. Wiley, Chichester.
- Otterlei, M., Warbrick, E., Nagelhus, T.A., Haug, T., Slupphaug, G., Akbari, M., Aas, P.A., Steinsbekk, K., Bakke, O., Krokan, H.E., 1999. Post-replicative base excision repair in replication foci. *EMBO J.* 18, 3834–3844.
- Press, W.H., Teukolsky, S.A., Vetterling, W.T., Flannery, B.P., 1999. *Numerical Recipes in C*. Cambridge University Press, Cambridge.
- Scheer, U., Weisenberger, D., 1994. The nucleolus. *Curr. Opin. Cell Biol.* 6, 354–359.
- Sparvoli, E., Levi, M., Rossi, E., 1994. Replicon clusters may form structurally stable complexes of chromatin and chromosomes. *J. Cell Sci.* 107, 3097–3103.
- Spector, D.L., 2001. Nuclear domains. *J. Cell Sci.* 114, 2891–2893.
- Sporbert, A., Gahl, A., Ankerhold, R., Leonhardt, H., Cardoso, M.C., 2002. DNA polymerase clamp shows little turnover at established replication sites but sequential de novo assembly at adjacent origin clusters. *Mol. Cell* 10, 1355–1365.
- Stein, G.S., Zaidi, S.K., Braastad, C.D., Montecino, M., van Wijnen, A.J., Choi, J.-Y., Stein, J.L., Lian, J.B., Javed, A., 2003. Functional architecture of the nucleus: organizing the regulatory machinery for gene expression, replication and repair. *Trends Cell Biol.* 13, 584–592.
- Tube, R.A., Berezney, R., 1987. Identification of 100 and 150 S DNA polymerase alpha-primase megacomplexes solubilized from the nuclear matrix of regenerating rat liver. *J. Biol. Chem.* 262, 5857–5865.
- van Driel, R., Fransz, P., 2004. Nuclear architecture and genome functioning in plants and animals: what can we learn from both?. *Exp. Cell Res.* 296, 86–90.
- Weibel, E.R., 1979. *Practical methods for biological morphometry*. *Stereological Methods*, vol. 1. Academic Press, London.
- Zink, D., Cremer, T., Saffrich, R., Fischer, R., Trendelenburg, M.F., Ansorge, W., Stelzer, E.H., 1998. Structure and dynamics of human interphase chromosome territories in vivo. *Hum. Genet.* 102, 241–251.